

Carbonic Acid: From Polyamorphism to Polymorphism

Katrin Winkel,[†] Wolfgang Hage,[†] Thomas Loerting,^{*,†,‡} Sarah L. Price,[§] and Erwin Mayer[†]

Contribution from the Institute of General, Inorganic, and Theoretical Chemistry and the Institute of Physical Chemistry, University of Innsbruck, A-6020 Innsbruck, Austria, and from the Department of Chemistry, University College London, 20 Gordon Street, London WC1H 0AJ, U.K.

Received May 18, 2007; E-mail: Thomas.Loerting@uibk.ac.at

Abstract: Layers of glassy methanolic (aqueous) solutions of KHCO₃ and HCl were deposited sequentially at 78 K on a CsI window, and their reaction on heating in vacuo in steps from 78 to 230 K was followed by Fourier transform infrared (FTIR) spectroscopy. After removal of solvent and excess HCl, IR spectra revealed formation of two distinct states of amorphous carbonic acid (H₂CO₃), depending on whether KHCO₃ and HCl had been dissolved in methanol or in water, and of their phase transition to either crystalline α - or β -H₂CO₃. The main spectral features in the IR spectra of α - and β -H₂CO₃ are observable already in those of the two amorphous H₂CO₃ forms. This indicates that H-bond connectivity or conformational state in the two crystalline phases is on the whole already developed in the two amorphous forms. The amorphous nature of the precursors to the two crystalline polymorphs is confirmed using powder X-ray diffraction. These diffractograms also show that α - and β -amorphous H₂CO₃ are two distinct structural states. The variety of structural motifs found within a few kJ/mol in a computational search for possible crystal structures provides a plausible rationalization for (a) the observation of more than one amorphous form and (b) the retention of the motif observed in the amorphous form in the corresponding crystalline form. The polymorphism inferred for carbonic acid from our FTIR spectroscopic and powder X-ray diffraction studies is special since two different crystalline states are linked to two distinct amorphous states. We surmise that the two amorphous states of H₂CO₃ are connected by a first-order-like phase transition.

Introduction

Carbonic acid (H₂CO₃), the short-lived intermediate in CO₂–HCO₃[−]/CO₃^{2−} proton-transfer reactions, is a key compound in biological and geochemical carbonate-containing systems.^{1–9} At ambient temperature, H₂CO₃ dissolved in water dissociates rapidly into CO₂ and H₂O, with a rate constant of ~ 20 s^{−1} and an activation enthalpy of ~ 70 kJ mol^{−1}; the reaction is highly exergonic.¹ Carbonic acid was long believed to be an unstable molecule decomposing rapidly into its constituents CO₂ and H₂O. However, in 1987, it had been detected in the gas-phase decomposition products of (NH₄)HCO_{3(s)} by observation of a peak at a mass-to-charge ratio (m/z) of 62 attributed to H₂CO₃⁺ and with an intensity $< 1\%$ of the CO₂⁺ peak at $m/z = 44$.¹⁰ Subsequently, carbonic acid has been synthesized at low

temperatures by two basically different routes: (1) high-energy irradiation of cryogenic CO₂/H₂O mixtures^{11–18} and proton irradiation of pure solid CO₂¹⁴ and (2) protonation of bicarbonate or carbonate in a new cryogenic technique developed by our group.^{19–24} Fourier-transform infrared (FTIR) spectroscopic studies led to characterization of two polymorphs. One (β -H₂CO₃) is formed by high-energy irradiation^{11–18} or by protonation in freeze-concentrated aqueous solution.^{20,21,23} The other

- [†] General, Inorganic, and Theoretical Chemistry, University of Innsbruck.
[‡] Institute of Physical Chemistry, University of Innsbruck.
[§] University College London.
- (1) Baczko, C. Kohlensäure H₂CO₃ und ihre Ionen. In *Gmelin Handbuch der anorganischen Chemie, Kohlenstoff*; Pietsch, E. H. E., Kotowski, A., Eds.; Verlag Chemie: Weinheim, Germany, 1973; Vol. 14, Teil C3, p 117.
 - (2) Kern, D. M. *J. Chem. Educ.* **1960**, *37*, 14.
 - (3) Eigen, M.; Kustin, K.; Maass, G. Z. *Phys. Chem.* **1961**, *30*, 130.
 - (4) Jönsson, B.; Karlström, G.; Wennerström, H.; Forsen, S.; Roos, B.; Almlöf, J. *J. Am. Chem. Soc.* **1977**, *99*, 4628.
 - (5) Pocker, Y.; Björkquist, D. W. *J. Am. Chem. Soc.* **1977**, *99*, 6537.
 - (6) Nguyen Minh, T.; Ha, T. K. *J. Am. Chem. Soc.* **1984**, *106*, 599.
 - (7) Nguyen, M. T.; Hegarty, A. F.; Ha, T. K. *THEOCHEM* **1987**, *35*, 319.
 - (8) Khanna, R. K.; Tossell, J. A.; Fox, K. *Icarus* **1994**, *112*, 541.
 - (9) Wight, C. A.; Boldyrev, A. I. *J. Phys. Chem.* **1995**, *99*, 12125.
 - (10) Terlouw, J. K.; Lebrilla, C. B.; Schwarz, H. *Angew. Chem.* **1987**, *99*, 352.

- (11) Moore, M. H.; Khanna, R. K. *Spectrochim. Acta, Part A: Mol. Biomol. Spectrosc.* **1991**, *47A*, 255.
- (12) Moore, M. H.; Khanna, R.; Donn, B. *J. Geophys. Res. [Planets]* **1991**, *96*, 17541.
- (13) DelloRusso, N.; Khanna, R. K.; Moore, M. H. *J. Geophys. Res.* **1993**, *98*, 5505.
- (14) Brucato, J. R.; Palumbo, M. E.; Strazzulla, G. *Icarus* **1997**, *125*, 135.
- (15) Gerakines, P. A.; Moore, M. H.; Hudson, R. L. *Astron. Astrophys.* **2000**, *357*, 793.
- (16) Strazzulla, G.; Baratta, G. A.; Palumbo, M. E.; Satorre, M. A. *Nucl. Instrum. Methods Phys. Res., Sect. B: Beam Interact. Mater. Atoms* **2000**, *166–167*, 13.
- (17) Moore, M. H.; Hudson, R. L.; Gerakines, P. A. *Spectrochim. Acta, Part A: Mol. Biomol. Spectrosc.* **2001**, *57A*, 843.
- (18) Wu, C. Y. R.; Judge, D. L.; Cheng, B.-M.; Yih, T.-S.; Lee, C. S.; Ip, W. H. *J. Geophys. Res. [Planets]* **2003**, *108*, 13/1.
- (19) Hage, W.; Hallbrucker, A.; Mayer, E. *J. Am. Chem. Soc.* **1993**, *115*, 8427.
- (20) Hage, W.; Hallbrucker, A.; Mayer, E. *J. Chem. Soc., Faraday Trans.* **1995**, *91*, 2823.
- (21) Hage, W.; Hallbrucker, A.; Mayer, E. *J. Chem. Soc., Faraday Trans.* **1996**, *92*, 3197.
- (22) Hage, W.; Hallbrucker, A.; Mayer, E. *J. Chem. Soc., Faraday Trans.* **1996**, *92*, 3183.
- (23) Hage, W.; Hallbrucker, A.; Mayer, E. *J. Mol. Struct.* **1997**, *408–409*, 527.
- (24) Hage, W.; Liedl, K. R.; Hallbrucker, A.; Mayer, E. *Science (Washington, DC, U.S.)* **1998**, *279*, 1332.

(α - H_2CO_3) is formed by protonation in methanolic solution,^{19,20,22–24} with β - H_2CO_3 transforming into α - H_2CO_3 on treatment with methanol/HCl.²⁰ We have shown experimentally that α - H_2CO_3 can be sublimated and recondensed without decomposition.²⁴ For the gas phase of H_2CO_3 , our high-level molecular quantum mechanical calculations show that hydrogen bonding stabilizes the dimer,²⁵ that water-free H_2CO_3 is kinetically very stable, with a half-life of about 180,000 years at ambient temperature,²⁶ and that it requires up to three water molecules to approach the experimental decomposition rate.²⁷ Since H_2O and CO_2 coexist in various astrophysical environments such as in icy grain mantles in the interstellar medium, the formation of solid or gaseous carbonic acid by high-energy irradiation and its astrophysical significance is being discussed.^{8,13,14,17,18,20,21,24,28–32} Recently, detection of carbonic acid adsorbed on calcium carbonate indicated that under ambient conditions, “carbonic acid may be an important albeit short-lived intermediate in the surface chemistry of calcium carbonate” on earth.^{33,34}

Here, we show by FTIR spectroscopy and X-ray diffraction that the two crystal polymorphs α - H_2CO_3 and β - H_2CO_3 are formed from two distinctly different amorphous states, indicating polyamorphism for H_2CO_3 . Polyamorphism is the term for having multiple distinct glassy states,³⁵ and it was observed for the first time in amorphous ice.^{36,37} Since then, many one-component types of systems showing multiple amorphous solids have been discovered (reviewed in refs 38–40). The polyamorphism inferred for carbonic acid from our FTIR spectroscopic and X-ray diffraction studies is special since two different crystalline states are linked to two distinct amorphous states. Recently, it has been reported that the amorphous calcium carbonate phase in larval snail shells has the short-range order of aragonite before it crystallizes,⁴¹ whereas the amorphous calcium carbonate phase transforming in sea urchin embryos into calcite has already the short-range order of calcite.^{42,43} It shows that organisms build their calcium carbonate skeletons starting with amorphous phases, with short-range order of the crystalline calcite or aragonite phases into which they are transforming. Thus, the concept of polyamorphism to polymorphism seems to be important in the biomineralization of calcium carbonate, suggesting that the process that we have observed

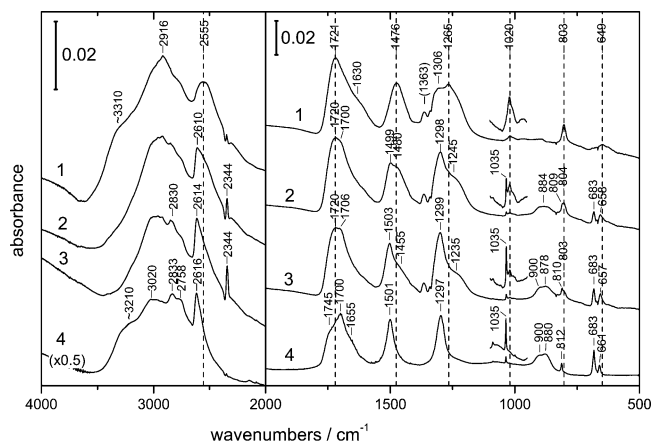


Figure 1. The amorphous \rightarrow β - H_2CO_3 phase transition as seen by the temperature dependence of a film made by reaction of aqueous solutions of KHCO_3 and HCl recorded on heating in vacuo at 200, 220, and 230 K (curves 1–3). Curve 4 shows for comparison the IR spectrum of a fully crystalline β - H_2CO_3 film made by reaction of KHCO_3 with HBr and recorded in vacuo at 200 K. Vertical dashed lines mark the peak positions of amorphous H_2CO_3 . The spectral region at $\sim 1020/1035$ cm^{-1} is also shown fourfold enhanced. In curves 1–3, the band at ~ 1363 cm^{-1} is from a nonvolatile impurity on the window. Curves 1–3 are shown on the same scale; curve 4 is reduced by a factor of 0.5. The sharp band at 2344 cm^{-1} in curves 2 and 3 is from enclosed CO_2 .

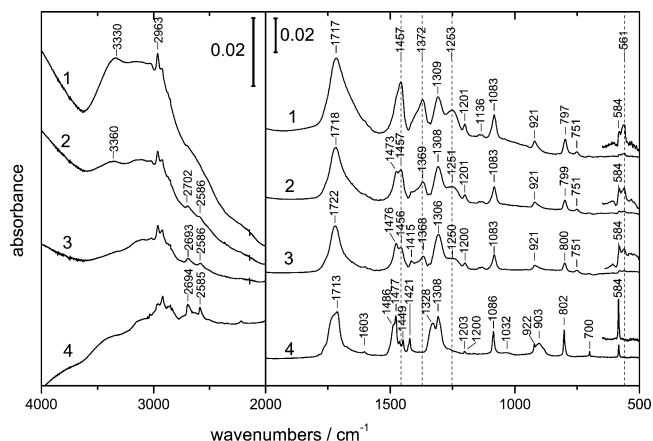


Figure 2. The amorphous \rightarrow α - H_2CO_3 phase transition as seen by the temperature dependence of a film made by reaction of methanolic solutions of KHCO_3 and HCl recorded on heating in vacuo at 190, 200, and 210 K (curves 1–3). Curve 4 shows for comparison the IR spectrum of a nearly fully crystalline α - H_2CO_3 film made also by reaction of methanolic solutions of KHCO_3 and HCl and recorded in vacuo at 200 K. Vertical dashed lines mark the peak positions of amorphous H_2CO_3 . The two-band region at $\sim 561/584$ cm^{-1} is also shown enhanced after smoothing of the spectra of curves 1–3. In curve 4, the weak band at 1032 cm^{-1} is from a trace of CH_3OH . Curves 1–4 are shown on the same scale. (Curve 4 is from Figure 1 in ref 24.)

for carbonic acid may help understand the formation of polymorphs in a wide range of systems.

Experimental Section

H_2CO_3 films were prepared on a CsI window by depositing sequentially at 78 K layers of glassy aqueous solutions of 0.1 M KHCO_3 and ~ 1 M HCl in the form of droplets for Figure 1 (~ 1 M HBr for curve 4) or of glassy methanolic solutions of 0.1 M KHCO_3 and ~ 1 M HCl for Figure 2. The deposits were then heated in vacuo from 78 to 200 K (190 K for Figure 2) to induce protonation of HCO_3^- and removal of solvent (H_2O or CH_3OH) and excess HCl . Removal of solvent, protonation of HCO_3^- , and phase transition to either α - or β - H_2CO_3 was followed by FTIR spectroscopy on further

- (25) Liedl, K. R.; Sekusak, S.; Mayer, E. *J. Am. Chem. Soc.* **1997**, *119*, 3782.
 (26) Loerting, T.; Tautermann, C.; Kroemer, R. T.; Kohl, I.; Hallbrucker, A.; Mayer, E.; Liedl, K. R. *Angew. Chem., Int. Ed.* **2000**, *39*, 892.
 (27) Tautermann, C. S.; Voegelé, A. F.; Loerting, T.; Kohl, I.; Hallbrucker, A.; Mayer, E.; Liedl, K. R. *Chem.–Eur. J.* **2002**, *8*, 66.
 (28) Lewis, J. S.; Grinspoon, D. H. *Science (Washington, DC, U.S.)* **1990**, *249*, 1273.
 (29) Strazzulla, G.; Brucato, J. R.; Palumbo, N. E. *Planet. Space Sci.* **1996**, *44*, 1447.
 (30) Delitsky, M. L.; Lane, A. L. *J. Geophys. Res. [Planets]* **1998**, *103*, 31391.
 (31) Strazzulla, G. *Planet. Space Sci.* **1999**, *47*, 1371.
 (32) Moore, M. H.; Hudson, R. L.; Ferrante, R. F. *Earth, Moon, Planets* **2004**, *92*, 291.
 (33) Al-Hosney, H. A.; Grassian, V. H. *J. Am. Chem. Soc.* **2004**, *126*, 8068.
 (34) Al-Hosney, H. A.; Grassian, V. H. *Phys. Chem. Phys.* **2005**, *7*, 1266.
 (35) Debenedetti, P. G.; Stanley, H. E. *Phys. Today* **2003**, 40.
 (36) Mishima, O.; Calvert, L. D.; Whalley, E. *Nature* **1984**, *310*, 393.
 (37) Mishima, O.; Calvert, L. D.; Whalley, E. *Nature* **1985**, *314*, 76.
 (38) Poole, P. H.; Grande, T.; Angell, C. A.; McMillan, P. F. *Science* **1997**, *275*, 322.
 (39) McMillan, P. F. *J. Mater. Chem.* **2004**, *14*, 1506.
 (40) Wilding, M. C.; Wilson, M.; McMillan, P. F. *Chem. Soc. Rev.* **2006**, *35*, 964.
 (41) Hasse, B.; Ehrenberg, H.; Marxen, J. C.; Becker, W.; Epple, M. *Chem. Eur. J.* **2000**, *6*, 3679.
 (42) Politi, Y.; Arad, T.; Klein, E.; Weiner, S.; Addadi, L. *Science* **2004**, *306*, 1161.
 (43) Politi, Y.; Levi-Kalishman, Y.; Raz, S.; Wilt, F.; Addadi, L.; Weiner, S.; Sagi, I. *Adv. Funct. Mater.* **2006**, *16*, 1289.

heating of the films in steps. IR spectra were recorded in transmission on Biorad's FTS 45 at 2 cm^{-1} resolution (UDR1) by coadding 256 scans. The spectrum of water vapor was subtracted from the spectra, but no other spectral manipulations were carried out. For further experimental details see ref 44.

The very weak band centered at 1032 cm^{-1} in curve 4 of Figure 2 is from a trace of CH_3OH . On request of reviewers, we used this band to estimate the minimum amount of CH_3OH which can be detected by FTIR spectroscopy and the relative amounts of H_2CO_3 to CH_3OH . This band assigned to the C–O stretching vibration is very intense in the IR spectrum of CH_3OH ,⁴⁵ and it is in a spectral region free of H_2CO_3 IR bands. This band was reported to be insensitive to the presence of water⁴⁶ or electrolytes.⁴⁷ For the following, it is important that this CH_3OH band shows little change in peak position and band shape in going from liquid CH_3OH at $\sim 300\text{ K}$ to CH_3OH in $\alpha\text{-H}_2\text{CO}_3$ preparations below 200 K . First, the IR spectrum of liquid CH_3OH (Aldrich, HPLC quality) was recorded in a calibrated liquid cell with $15.6\text{ }\mu\text{m}$ path length. Thereafter, fractional amounts of this spectrum were coadded to spectra of $\alpha\text{-H}_2\text{CO}_3$ free of the band at 1032 cm^{-1} (using Origin 7.5), for example, curve 1 in Figure 2, to determine the minimal amount of CH_3OH which is detectable. Addition of a fraction of 0.0002 to the latter $\alpha\text{-H}_2\text{CO}_3$ spectrum is clearly observable by intensity increase. This corresponds to an average CH_3OH thickness of $\sim 3\text{ nm}$. The weak CH_3OH band in curve 4 of Figure 2 then is estimated to have an average thickness of $\sim 6\text{ nm}$. Second, the amount of H_2CO_3 formed on protonation of HCO_3^- was determined, as outlined in footnote 17 of ref 24, by comparison of band areas. Deuterated solvents were chosen because then the KDCO_3 band at 1632 cm^{-1} does not contain contributions from other bands (for example, the OH deformation mode). For this comparison, spectra depicted in Figure 1b of ref 19 as curves 1 and 5 were selected because the 1:1 correspondence between D_2CO_3 and DCO_3^- was established by quantitative conversion and the absence of CO_2 . Band area ratio was 0.33 for $\nu\text{C}=\text{O}$ (in D_2CO_3)/ $\nu\text{C}=\text{O}$ (in DCO_3^-). Thereafter, absorbance of the KHCO_3 band was determined in a calibrated liquid cell ($15.0\text{ }\mu\text{m}$ path length) for 0.10 M KHCO_3 dissolved in CH_3OH . From KHCO_3 concentration and path length, an average thickness of $\sim 0.10\text{ }\mu\text{m}$ is calculated for solid KHCO_3 of density 1.5 g cm^{-3} . Band area of the KDCO_3 band, curve 1 in Figure 1b,¹⁹ is slightly smaller which results in an average thickness of $\sim 0.085\text{ }\mu\text{m}$. By comparison with formic acid's density of 1.22 g cm^{-3} , we assume for H_2CO_3 a slightly higher density of 1.3 g cm^{-3} . This then gives for curve 5 of Figure 1b in ref 19 an average thickness of $\sim 0.10\text{ }\mu\text{m}$. This estimate can be used for estimations of the average thickness of $\alpha\text{-H}_2\text{CO}_3$ in other experiments by considering the relative heights of the C=O stretching vibrations (assuming similar band shapes). The height of the $\alpha\text{-D}_2\text{CO}_3$ band used for the estimation (curve 5 in Figure 1b of ref 19) is similar to that shown as curve 4 in Figure 2, about 0.03 absorbance units. These are typical values in most of our experiments; only in a few experiments were we able to obtain an about fivefold intensity by multilayer deposits. In a third step, for curve 4 of our Figure 2, this average thickness of $\alpha\text{-H}_2\text{CO}_3$ of $\sim 0.10\text{ }\mu\text{m}$, or 100 nm , can be compared with the average CH_3OH thickness of $\sim 6\text{ nm}$ obtained as described above. Considering the differences in densities (and assuming a density of 0.80 for CH_3OH and of 1.3 for H_2CO_3), the $\text{H}_2\text{CO}_3/\text{CH}_3\text{OH}$ molar ratio is ~ 14 . For curve 1 of Figure 2, where no CH_3OH band can be detected at 1032 cm^{-1} , the $\text{H}_2\text{CO}_3/\text{CH}_3\text{OH}$ molar ratio must be higher: from the CH_3OH detection limit of $\sim 3\text{ nm}$ (see above), we estimate it to be at least ~ 28 . $\beta\text{-H}_2\text{CO}_3$ solvent impurity could not be estimated in this manner because the solvent water does not have a suitable sharp IR band.

X-ray diffractograms were recorded on a diffractometer in $\theta\text{-}\theta$ geometry (Siemens, model D 5000, Cu–K α), equipped with a low-temperature camera from Paar. The sample plate was in horizontal position during the whole measurement. Installation of a "Goebel mirror" allowed to record small amounts of sample without distortion of the Bragg peaks. To obtain sufficient intensity, the procedure had to be modified: samples were prepared by freezing of droplets (about 1 mm in diameter) of the solutions in liquid nitrogen, which were then pestled in a glass mortar at 77 K and were transferred to the X-ray sample holder. For preparation of $\alpha\text{-H}_2\text{CO}_3$, methanolic solutions of 0.1 M KHCO_3 and $\sim 1\text{ M HBr}$ were quenched separately in liquid nitrogen; for $\beta\text{-H}_2\text{CO}_3$, aqueous solutions of 1 M KHCO_3 and $\sim 4\text{ M HBr}$ were quenched. The pestled starting materials were slowly heated in vacuo ($5\cdot 10^{-4}\text{ mbar}$) for inducing protonation of KHCO_3 and pumping off the solvents methanol and water and excess HBr.

MOLPAK⁴⁸ was used to search for the low-energy, $Z' = 1$, crystal structures of the MP2 6-31G** optimized rigid conformers of carbonic acid. The lattice energy, calculated from the distributed multipole analysis of this ab initio charge density and an empirical atom–atom repulsion model,⁴⁹ was minimized using DMAREL.⁵⁰ The crystal symmetry was reduced until a stable minimum was found, generating some structures with $Z' > 1$. More extensive searches using the expected hydrogen-bonded dimers (i.e., two monomers starting in this geometry) as the crystal building unit were also performed. Unfortunately, more accurate calculations of the relative crystal energies are not currently possible as the adjustment of the molecular conformations in response to the packing forces is too demanding of correctly modeling the balance between the various inter- and intramolecular hydrogen bonding and dispersion forces.

Results

Phase Transitions Followed by FTIR Spectroscopy. We first show how the IR spectrum of $\beta\text{-H}_2\text{CO}_3$ develops on heating an amorphous H_2CO_3 film in vacuo (Figure 1). The film was obtained by reaction of aqueous solutions of $\sim 0.1\text{ M KHCO}_3$ and $\sim 1\text{ M HCl}$. Curve 1 recorded at 200 K is attributed to mainly amorphous H_2CO_3 , and curves 2 and 3 recorded at 220 and 230 K show how the spectrum of $\beta\text{-H}_2\text{CO}_3$ develops from that of amorphous H_2CO_3 . For assignment of the IR bands of $\beta\text{-H}_2\text{CO}_3$ in terms of a qualitative description of the modes, see Tables 1 in refs 21 and 13. Vertical dashed lines mark the peak positions of amorphous H_2CO_3 . The sloping background between 4000 and $\sim 3500\text{ cm}^{-1}$ in this and the following figures is caused by the Christiansen effect.⁵¹

The spectral changes are characteristic for an amorphous-to-crystalline phase transition (reviewed in ref 52). These are in particular shift of peak maxima, narrowing and splitting of bands in a narrow temperature region, and several examples are discussed as follows. First, the intense band centered in curve 1 at 2555 cm^{-1} shifts on crystallization to 2614 cm^{-1} (curve 3). The latter band had been assigned to the overtone of the in-plane (COH) bending mode centered at 1302 cm^{-1} (Table 1 in ref 21). The appearance of a broad band at $\sim 1265\text{ cm}^{-1}$ in curve 1 is consistent with the assignment; its intensity decreases and develops to a shoulder on heating and phase transition. Second, the broad band centered in curve 1 at 1476 cm^{-1} shifts to 1503 cm^{-1} in curve 3 (assigned to the antisymmetric $\text{C}(\text{OH})_2$ stretching mode). Third, sharp bands centered at 683 and 657

(44) Hage, W.; Hallbrucker, A.; Mayer, E. *J. Chem. Soc., Faraday Trans.* **1996**, *92*, 3183.

(45) Herzberg, G. *Molecular Spectra and Structure II. Infrared and Raman Spectra of Polyatomic Molecules*; van Nostrand: New York, 1945.

(46) Yang, R. T.; Low, M. J. D. *Spectrochim. Acta* **1974**, *30A*, 1787.

(47) Al-Baldawi, S. A.; Brooker, M. H.; Gough, T. E.; Irish, D. E. *Can. J. Chem.* **1970**, *48*, 1202.

(48) Holden, J. R.; Du, Z. Y.; Ammon, H. L. *J. Comput. Chem.* **1993**, *14*, 422.

(49) Coombes, D. S.; Price, S. L.; Willock, D. J.; Leslie, M. *J. Phys. Chem.* **1996**, *100*, 7352.

(50) Willock, D. J.; Price, S. L.; Leslie, M.; Catlow, C. R. A. *J. Comput. Chem.* **1995**, *16*, 628.

(51) Bertie, J. E.; Whalley, E. *J. Chem. Phys.* **1964**, *40*, 1637.

cm^{-1} (curve 3, in-plane (CO_3) bending mode) develop from the broad band at $\sim 649 \text{ cm}^{-1}$ (curve 1). Fourth, the weak broad band centered in curve 1 at $\sim 1020 \text{ cm}^{-1}$ shifts in curve 3 on crystallization to a sharp band centered at 1035 cm^{-1} . The latter band had been assigned to the symmetric $\text{C}(\text{OH})_2$ stretching mode. This band system seems to consist of two bands only, a broad one at $\sim 1020 \text{ cm}^{-1}$ from the amorphous phase and a sharp one at 1035 cm^{-1} from $\beta\text{-H}_2\text{CO}_3$, and therefore it is very useful in estimating relative amounts of amorphous and crystalline phase. Curve 3 contains a minor broad feature at $\sim 1020 \text{ cm}^{-1}$ which indicates that even on heating to 230 K crystallization is not complete.

These results are consistent with our previous findings that on protonation of KHCO_3 with HCl , amorphous H_2CO_3 is first formed which slowly converts with increasing temperature to $\beta\text{-H}_2\text{CO}_3$.²¹ However, this conversion is not complete, even at the highest temperatures. On the other hand, on protonation of KHCO_3 with HBr , a fully crystalline film is immediately obtained. Therefore, we show as curve 4 the IR spectrum of a film of $\beta\text{-H}_2\text{CO}_3$ made by protonation of KHCO_3 with HBr : in this spectrum, the features of amorphous H_2CO_3 , as defined above, are now absent. In particular, the broad band at $\sim 1020 \text{ cm}^{-1}$ attributed to amorphous H_2CO_3 is now absent and the sharp band at 1035 cm^{-1} from $\beta\text{-H}_2\text{CO}_3$ is very intense.

While most of the band systems show gradual changes in going from the amorphous to the fully crystalline state (curve 1 to 4), the broad shoulder at $\sim 3310 \text{ cm}^{-1}$ in curve 1 and at $\sim 3210 \text{ cm}^{-1}$ in curve 4 is an exception because it is not observable in curves 2 and 3. This shoulder had been assigned to an overtone of the $\text{C}=\text{O}$ stretching vibration ($\nu \text{C}=\text{O}$).²¹ In carboxylic acids generally, the occurrence of subpeaks superimposed on the broad and intense $\text{O}-\text{H}$ stretching band region ($\nu \text{O}-\text{H}$) has been ascribed to Fermi resonance effects where the intensity of combination bands or overtones is enhanced by interaction with $\nu \text{O}-\text{H}$.⁵³⁻⁵⁶ Thus, it seems reasonable to attribute also in curves 1 and 4 the intensity of the shoulders to Fermi resonance. On phase transition from amorphous to $\beta\text{-H}_2\text{CO}_3$, $\nu \text{O}-\text{H}$ narrows and the shoulder shifts from $\sim 3310 \text{ cm}^{-1}$ in curve 1 to $\sim 3210 \text{ cm}^{-1}$ in curve 4. This decrease is consistent with decreasing $\nu \text{C}=\text{O}$ peak frequency in going from the amorphous state (curve 1, 1721 cm^{-1}) to the crystalline state (curve 4, 1700 cm^{-1}). Band narrowing by second-derivative curves further shows that the two shoulders are caused by different subbands (not shown). The question remains why the shoulder is not observable anymore in curves 2 and 3. These spectra contain varying amounts of amorphous/crystalline H_2CO_3 , and superposition of the two broad shoulders is expected to lead to further broadening and so the shoulders could become unobservable. In addition, changes of the $\nu \text{O}-\text{H}$ peak shape on crystallization can lead to decrease in intensity enhancement by Fermi resonance.⁴⁵

In the same manner, we show how the IR spectrum of $\alpha\text{-H}_2\text{CO}_3$ develops on heating an amorphous H_2CO_3 film in

vacuo (Figure 2). The film was obtained by reaction of methanolic solutions of $\sim 0.1 \text{ M KHCO}_3$ and $\sim 1 \text{ M HCl}$. Curve 1 recorded at 190 K is attributed to mainly amorphous H_2CO_3 with the broad peak in the $\text{O}-\text{H}$ stretching band region originating from traces of included ice. Curves 2 and 3 recorded at 200 and 210 K show how the spectrum of $\alpha\text{-H}_2\text{CO}_3$ develops from that of amorphous H_2CO_3 . For assignment of the IR bands of $\alpha\text{-H}_2\text{CO}_3$, see Table 1 in ref 22. Vertical dashed lines mark the peak positions of amorphous H_2CO_3 , and the spectral changes on phase transition to $\alpha\text{-H}_2\text{CO}_3$ are pointed out as follows. First, the IR band centered in curve 1 at 1457 cm^{-1} shifts on crystallization to 1476 cm^{-1} (curve 3, assigned to antisymmetric $\text{C}(\text{OH})_2$ stretching vibration). Second, the bands at 1372 and $\sim 1253 \text{ cm}^{-1}$ (curve 1) decrease in intensity (curves 2 and 3), and the band centered in curve 1 at 1717 cm^{-1} ($\text{C}=\text{O}$ stretching vibration) narrows considerably in particular at lower wavenumbers in curves 2 and 3. Third, the two weak bands at 2693 and 2586 cm^{-1} in curve 3 (at 2702 and 2586 cm^{-1} in curve 2) had been assigned to $\text{O}-\text{H}$ stretching vibrations, in accordance with the spectral positions in the $\alpha\text{-H}_2^{13}\text{CO}_3$ and $\alpha\text{-D}_2\text{CO}_3$ isotopomers (see Table 1 in ref 22). These peaks are not observable in curve 1, apparently because of band broadening. Fourth, a very weak two-band system consisting of a broad band at $\sim 561 \text{ cm}^{-1}$ and a sharp one at 584 cm^{-1} (shown enhanced) allows to follow the phase transition from amorphous H_2CO_3 (band at $\sim 561 \text{ cm}^{-1}$) to $\alpha\text{-H}_2\text{CO}_3$ (band at 584 cm^{-1} , assigned to in-plane (CO_3) bending mode) by the changes in relative intensity from curves 1-3. This two-band system also shows that curve 1 contains already a minor amount of $\alpha\text{-H}_2\text{CO}_3$ and that crystallization is not complete on heating to 210 K (curve 3).

According to the criteria for the presence of amorphous H_2CO_3 listed above, the crystallinity of $\alpha\text{-H}_2\text{CO}_3$ varies considerably depending on experimental details. This is indicated by the IR spectra reported in refs 19, 22, and 24. Therefore, we show as curve 4 the IR spectrum of a film of $\alpha\text{-H}_2\text{CO}_3$ made in the same manner by reaction of methanolic solutions of KHCO_3 and HCl and recorded in vacuo at 200 K. The high crystallinity of the film is indicated by further sharpening of bands and band splitting in comparison to curve 3, for example, the band centered in curve 3 at 1306 cm^{-1} with a shoulder at higher frequency (in the second derivative) splits in curve 4 into two bands at 1308 and 1328 cm^{-1} . According to the criteria for amorphous H_2CO_3 listed above, only a minor amount of amorphous H_2CO_3 is indicated in curve 4 by some residual intensity at $\sim 1250 \text{ cm}^{-1}$ and some tailing of the band centered at 1713 cm^{-1} . This spectrum further shows a trace of CH_3OH by the weak band at 1032 cm^{-1} . This film had been used in our sublimation and recondensation experiment of $\alpha\text{-H}_2\text{CO}_3$, and its IR spectrum is depicted in Figure 1 of ref 24 as curve 1. The IR spectrum of sublimated and recondensed $\alpha\text{-H}_2\text{CO}_3$ shown in the same reference as curve 2 is nearly identical with that of the film before sublimation and recondensation except that now the two features from a minor amount of amorphous H_2CO_3 and the weak peak from CH_3OH had disappeared.

We next compare the IR spectra of the two amorphous forms with those of α - and $\beta\text{-H}_2\text{CO}_3$ (Figure 3). Curves 1 and 2 are the IR spectra of the amorphous forms of H_2CO_3 obtained on reaction of methanolic solutions (curve 1) or aqueous solutions (curve 2) of KHCO_3 with HCl . Curve 3 is the IR spectrum of

(52) Bulkin, B. J. *Vibrational Spectroscopy for the Study of Order-Disorder Phenomena in Organic Materials*. In *Chemical, Biological and Industrial Applications of Infrared Spectroscopy*; Durig, J. R., Ed.; Wiley: New York, 1986; p 139.

(53) Bratoz, S.; Hadzi, D.; Sheppard, N. *Spectrochim. Acta* **1956**, *8*, 249.

(54) Bellamy, L. J.; Pace, R. J. *Spectrochim. Acta* **1963**, *19*, 435.

(55) Marechal, Y. *Infrared Spectra of Cyclic Dimers of Carboxylic Acids: The Mechanics of H-Bonds and Related Problems*. In *Vibrational Spectra and Structure*, 1987; Vol. 16, p 311.

(56) Wolfs, I.; Desseyn, H. O. *Appl. Spectrosc.* **1996**, *8*, 1000.

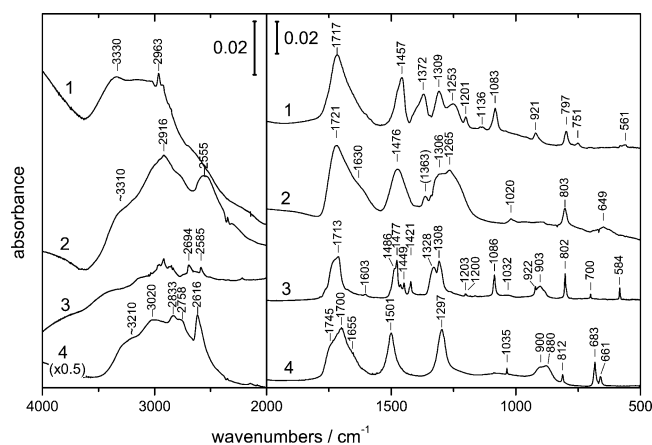


Figure 3. Comparison of IR spectra of the two amorphous states (curves 1 and 2) with those of α - and β - H_2CO_3 (curves 3 and 4). Curves 1 and 2 are curves 1 in Figures 1 and 2, and curves 3 and 4 are curves 3 and 4 in Figures 1 and 2.

α - H_2CO_3 , and curve 4 is that of β - H_2CO_3 . It is obvious that the IR spectra of the two amorphous forms (curves 1 and 2) differ in the same manner as those of the two crystalline forms (curves 3 and 4). Furthermore, the spectral pattern observable in the IR spectra of the crystalline forms is apparent already in those of the amorphous forms. This is particularly clear for amorphous and crystalline β - H_2CO_3 in curves 2 and 4. Phase transition from amorphous H_2CO_3 to β - H_2CO_3 further involves shift of several IR bands to higher wavenumbers, for example, $2555 \rightarrow 2616 \text{ cm}^{-1}$, $1476 \rightarrow 1501 \text{ cm}^{-1}$, $1265 \rightarrow 1297 \text{ cm}^{-1}$, $1020 \rightarrow 1035 \text{ cm}^{-1}$, and $649 \rightarrow 661/683 \text{ cm}^{-1}$. For the phase transition from amorphous H_2CO_3 to α - H_2CO_3 (curves 1 and 3), the IR spectra also show similar patterns, with shift of IR bands to higher wavenumbers on crystallization, for example, $1457 \rightarrow 1477/1486 \text{ cm}^{-1}$, $\sim 1253 \rightarrow 1308/1328 \text{ cm}^{-1}$, and $\sim 561 \rightarrow 584 \text{ cm}^{-1}$. These distinct amorphous states of H_2CO_3 are called in the following α -amorphous H_2CO_3 (curve 1) and β -amorphous H_2CO_3 (curve 2).

We summarize that demonstration of the amorphous-to-crystalline H_2CO_3 phase transition is tricky for both α - and β - H_2CO_3 . First, the extent of crystallization depends on several factors. For example, the reaction of aqueous solutions of KHCO_3 and HBr proceeds quickly and directly to β - H_2CO_3 , and amorphous H_2CO_3 cannot be identified. However, with HCl the reaction occurs much more slowly; amorphous H_2CO_3 can be characterized, but crystallization stops before conversion of amorphous H_2CO_3 to β - H_2CO_3 is complete (see Figure 1). This has been discussed, but not understood, in ref 21. Second, it is difficult to pump off the solvent in vacuo and to obtain IR spectra of amorphous H_2CO_3 without significant crystallization. This turned out to be a problem for reaction of methanolic solutions. CH_3OH has a very intense peak at $\sim 1030 \text{ cm}^{-1}$, and the absence of this peak in curves 1–3 of Figure 2 indicates that the film does not contain CH_3OH anymore. We have obtained additional IR spectral evidence for the two amorphous-to-crystalline H_2CO_3 phase transitions of the isotopomers $\text{H}_2^{13}\text{CO}_3$ and D_2CO_3 which are not shown here. We note that KCl , which is the second reaction product in the protonation of KHCO_3 with HCl , seems to have only a very minor influence on the extent of crystallization from methanolic solutions. This is demonstrated by Figure 1 in ref 24, where the IR spectrum of a film of α - H_2CO_3 containing KCl (curves 1, before

sublimation) is compared with that of the film of α - H_2CO_3 without KCl (curves 2, after sublimation and recondensation).

X-ray Diffractograms of the Two Amorphous Forms of H_2CO_3 . We further show X-ray diffractograms of α -amorphous and β -amorphous H_2CO_3 (Figure 4). The samples were made by reaction of KHCO_3 with HBr in methanolic solution for α -amorphous H_2CO_3 (a) and in aqueous solution for β -amorphous H_2CO_3 (c). In both cases, KBr is one of the reaction products on heating to 200 K (a) or 210 K (c), and the reflections of crystalline KBr are marked by open circles.⁵⁷ The other reaction product on protonation of HCO_3^- , H_2CO_3 , is attributed to broad peaks centered at $2\theta \sim 26^\circ$ in a and at $2\theta \sim 27^\circ$ in c, and the broadness of these peaks indicates that H_2CO_3 is amorphous. These broad peaks are superimposed by sharp peaks from hexagonal ice (marked by asterisks) and the substrate (full triangles). The broad peak attributed to β -amorphous H_2CO_3 (c) is clearly broader than that of α -amorphous H_2CO_3 (a), and its peak maximum is shifted slightly to higher 2θ values. Both broad peaks disappear on heating to 300 K in vacuo as expected for both forms of H_2CO_3 (Figure 4, b and d),^{11,19,21,22} and only the reflections of crystalline KBr and the substrate remain. We emphasize that reflections of the starting material KHCO_3 were not observable at 200 or 300 K, indicating that its protonation must have gone to completion. We further note that we did observe onset of crystallization of α -amorphous H_2CO_3 (β -amorphous H_2CO_3) by the appearance of sharp Bragg peaks when the sample was kept over hours at 200 K (210 K) (not shown) or slightly above these temperatures. These ongoing studies of X-ray diffraction patterns of α - and β - H_2CO_3 will be reported separately.

Discussion

Vibrational spectroscopy is an established technique for following phase transitions and for studies of polymorphism (reviewed in refs 58 and 59). Studies of polyamorphism by vibrational spectroscopy are more recent, and they concentrated on the high- and low-density forms of amorphous water.^{60–63} The polyamorphism shown in Figures 1–3 for H_2CO_3 is special since two different crystalline states are linked to the two different amorphous states. These FTIR spectroscopic studies are corroborated by X-ray diffractograms (Figure 4). It shows, therefore, that in carbonic acid polyamorphism leads directly to polymorphism. It indicates that the two amorphous states are separated by potential energy barriers which are higher than those to their crystalline states. It is conceivable that this type of behavior is much more general and that it occurs in many other systems (e.g., in calcium carbonate, see Introduction). However, it will often only be observable if the amorphous forms are made by a low-temperature technique, such as that used for H_2CO_3 , so that on heating structural changes caused by the amorphous \rightarrow crystalline phase transition can be followed.

(57) Meisalo, V.; Inkinen, O. *Acta Crystallogr.* **1967**, *22*, 58.

(58) Sherman, W. F.; Wilkinson, G. R. Raman and Infrared Studies of Crystals at Variable Pressure and Temperature. In *Advances in Infrared and Raman Spectroscopy*; Clark, R. J. H., Hester, R. E., Eds.; Heyden: London, 1980; Vol. 6, p 158.

(59) Iqbal, Z.; Owens, F. J. *Vibrational Spectroscopy of Phase Transitions*; Academic Press: London, 1984.

(60) Klug, D. D.; Mishima, O.; Whalley, E. *J. Chem. Phys.* **1987**, *86*, 5323.

(61) Mishima, O.; Suzuki, Y. *Nature* **2002**, *419*, 599.

(62) Tse, J. S.; Klug, D. D.; Tulk, C. A.; Svensson, E. C.; Swainson, I.; Shpakov, V. P.; Belosludov, V. R. *Phys. Rev. Lett.* **2000**, *85*, 3185.

(63) Loerting, T.; Salzmann, C.; Kohl, I.; Mayer, E.; Hallbrucker, A. *Phys. Chem. Chem. Phys.* **2001**, *3*, 5355.

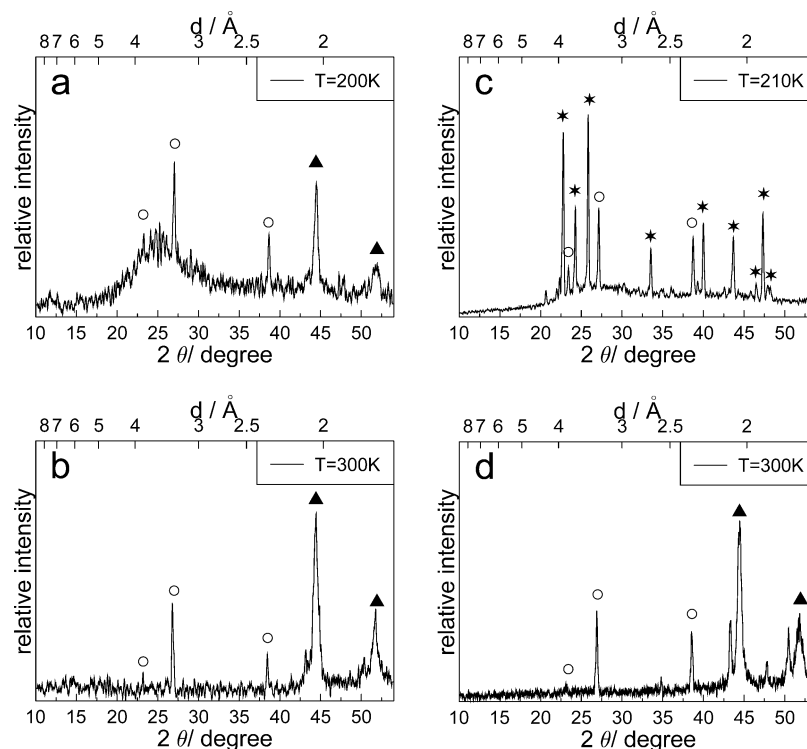


Figure 4. X-ray diffractograms (Cu–K α) (a) of the reaction products of 0.1 M KHCO₃ with \sim 1 M HBr in methanolic solution recorded after heating in vacuo from 77 to 200 K, the broad peak centered at \sim 26° is attributed to α -amorphous H₂CO₃, and (b) recorded on subsequent heating to 300 K, which causes H₂CO₃ to be pumped off. (c) of the reaction products of 1 M KHCO₃ with \sim 4 M HBr in aqueous solution recorded after heating in vacuo to 210 K, the broad peak centered at \sim 27° is attributed to β -amorphous H₂CO₃, and (d) recorded on subsequent heating to 300 K which causes H₂CO₃ to be pumped off. Bragg peaks in a–d from crystalline KBr are marked by open circles;⁵⁷ Bragg peaks from hexagonal ice in c are marked by asterisks and from the substrate in a, b, and d by full triangles.

We expect to find it in substances where molecules form a variety of hydrogen-bonded structures of varying energies.

H₂CO₃ is a dicarboxylic acid. For small carboxylic acids, the dimer and the catemer are the preferred hydrogen-bonding motifs.⁶⁴ The structures of α - and β -H₂CO₃ are not known, and it will be very difficult to obtain sufficient sample for determination of their structures by diffraction. However, it is obvious that in addition to crystal field and packing effects, the conformational flexibility of H₂CO₃ has to be considered because, as pointed out by Bernstein and Hagler, “in most cases energy differences between polymorphs do not exceed 2–3 kcal mol^{−1}, which is also the energy domain for torsional conformation parameters in many organic molecules. This suggests the possibility that molecules with torsional degrees of freedom may adopt different conformations in different polymorphs, a phenomenon known as conformational polymorphism”.^{65,66}

Thus, the monomer conformation of H₂CO₃ is an important factor for crystal packing. Numerous calculations for the formation of the H₂CO₃ monomer from gaseous H₂O and CO₂ have been performed at various levels, and they agree that the anti–anti conformer (i.e., both hydrogens point toward the carbonyl oxygen) is the most stable conformation and that the syn–anti conformer is only slightly less stable.^{67,69} High-level molecular quantum calculations of the H₂CO₃ dimer made from two anti–anti monomers indicated that this dimer is

remarkably stable and that the energy difference between the dimer and the constituents H₂O and CO₂ is, after correction for zero-point energy differences, “astonishingly close to zero”.^{24,25} Thus, the dimer and higher H₂CO₃ clusters^{68,69} have to be considered as building blocks in the crystal structures of α - and β -H₂CO₃.

We emphasize that the main spectral features in the IR spectra of α - and β -H₂CO₃ are observable already in those of the two amorphous H₂CO₃ forms (see Figure 3). This indicates that H-bond connectivity or conformational state in the two crystalline phases is on the whole already developed in the two amorphous forms. Thus, the determination of the possible crystal structures will show the possible short-range/intermediate-range motifs of the two H₂CO₃ amorphs.

Search for Hydrogen-Bonding Motifs in Amorphous H₂CO₃. The existence of amorphous phases of carbonic acid is not surprising given that there are a vast number of ways of packing this molecule in the solid state within a small energy range. Our simple search for crystal structures of the anti–anti conformer had four different stackings of the hydrogen-bonded sheet shown in Figure 5a within 1 kJ mol^{−1} of the global minimum in the lattice energy plus an alternative motif with three-dimensional hydrogen bonding (Figure 5b). Thus, stacking errors in growth with some regions of 3D hydrogen bonding seem highly likely⁷⁰ with the small energy differences between interchangeable motifs promoting the amorphous phase. A similar search with the syn–anti conformer also had many low-energy structures, including two different stackings of a sheet containing the doubly hydrogen-bonded motif (Figure 5c) and an alternative layer structure (Figure 5d) within a kJ mol^{−1} of

(64) Beyer, T.; Price, S. L. *J. Phys. Chem. B* **2000**, *104*, 2647.

(65) Bernstein, J.; Hagler, A. T. *J. Am. Chem. Soc.* **1978**, *100*, 673.

(66) Bernstein, J.; Hagler, A. T. *Mol. Cryst. Liq. Cryst.* **1979**, *50*, 223.

(67) Janoschek, R.; Csizmadia, I. G. *J. Mol. Struct.* **1993**, *300*, 637.

(68) Ballone, P.; Montanari, B.; Jones, R. O. *J. Chem. Phys.* **2000**, *112*, 6571.

(69) Tossell, J. A. *Inorg. Chem.* **2006**, *45*, 5961.

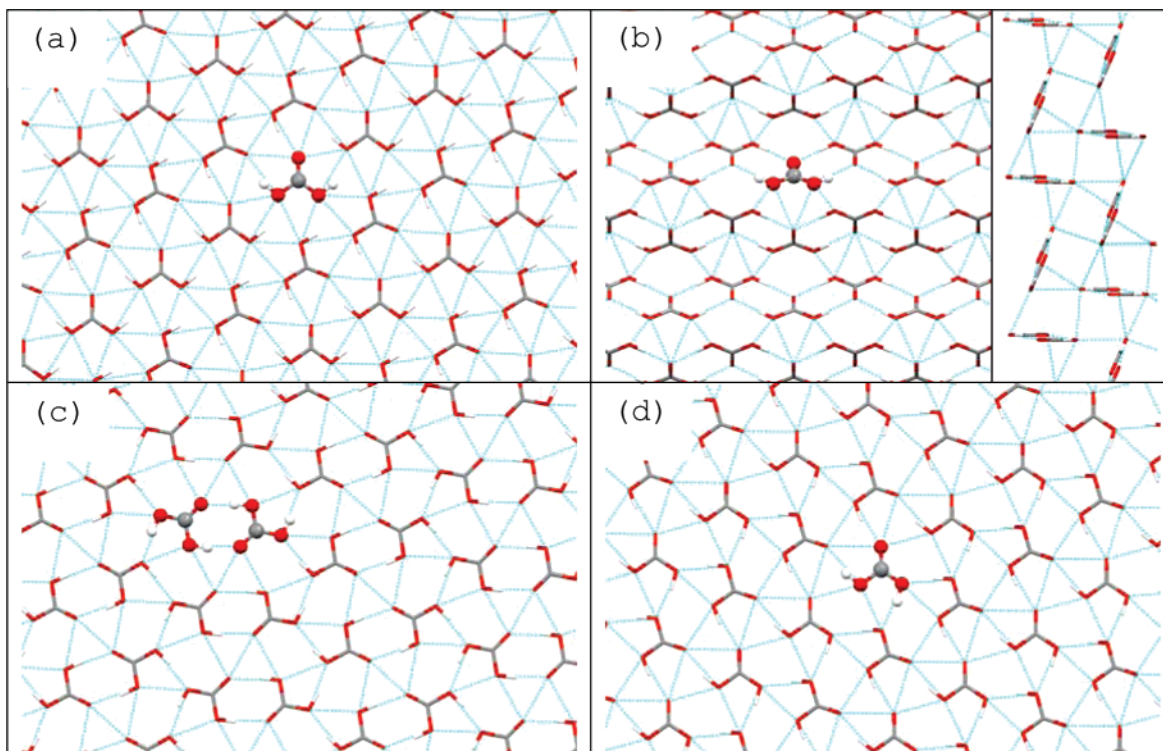


Figure 5. Hydrogen-bonding motifs from low-energy structures found for (top) anti–anti and (bottom) anti–syn carbonic acid. (a) The hydrogen-bonded sheet structure found in four low-energy structures (ak11, $P2_1/c$ $Z' = 1$ at -81.80 kJ/mol; av11 Pc $Z' = 2$ at -81.56 kJ/mol; ai10, $P2_1/c$ at -81.28 kJ/mol; cc46 $Pbca$ at -81.27 kJ/mol; and fc48 $P2_1/c$ at -80.99 kJ/mol). (b) A 3D hydrogen-bonded structure, bi8 $P1Z = 4$ at -81.24 kJ/mol. (c) The hydrogen-bonded sheet containing the anti–syn doubly hydrogen-bonded dimer, found, for example, in b22, $P2_1$ $Z' = 2$ at -84.10 kJ/mol and in al35 Pc $Z' = 2$ at -83.19 kJ/mol. (d) An alternative sheet without the dimer, ak35 $P2_1/c$ at -83.15 kJ/mol. Blue-dashed lines indicate hydrogen bonds as defined by the default lengths in Mercury.⁸⁴

its global minimum. This also suggests that crystallization into an ordered structure would be prone to growth errors. Since the syn–anti conformer gave slightly lower lattice energies than the anti–anti conformer, this would partially compensate for the higher conformational energy, making polymorphs of either conformer energetically feasible. Thus, a plausible rationalization of our observations is that the two sets of reaction conditions generate different conformations of the molecule as the growth units of the solid phase, possibly through the different solvation clusters formed in water or methanol. Either growth unit would readily form an amorphous phase because of the variety of locally ordered hydrogen-bonded sheets and 3D networks that can be formed. Since the barriers to changing an anti to syn conformation within the amorphous solid state would be greater than those involved in correcting growth mistakes such as misstackings of layers, the conformers would be maintained in the transformation to the ordered polymorph.

Solvent Effect on Carbonic Acid’s Polyamorphism and Polymorphism. We next discuss the effect of solvent on carbonic acid’s polyamorphism and polymorphism. As shown above (Figure 1), protonation of HCO_3^- in freeze-concentrated

aqueous solution leads to formation of first β -amorphous H_2CO_3 which then crystallizes to β - H_2CO_3 , whereas protonation of HCO_3^- in methanolic solution (Figure 2) gives first α -amorphous H_2CO_3 which crystallizes to α - H_2CO_3 . Protonation of HCO_3^- in methanol–water solution made by mixing equal volumes (56 wt % water) leads to formation of α -amorphous H_2CO_3 which does not crystallize anymore (see Figure 5, curve 1, in ref 22). β - H_2CO_3 can be transformed into α -amorphous H_2CO_3 on treatment with methanol/HCl (Figure 3 in ref 20). Thus, we obviously have a directing effect of the solvent, methanol or water, on the formation of the two amorphous and crystalline forms. A special case is the sublimation and recondensation experiment of α - H_2CO_3 where a trace of CH_3OH is observable by the very weak peak centered at 1032 cm^{-1} (Figure 1, curve 1, in ref 24) which is absent after condensation (curve 2). The $\text{H}_2\text{CO}_3/\text{CH}_3\text{OH}$ molar ratio of this trace amount is estimated as ~ 14 (see Experimental Section). Whether or not this CH_3OH impurity has a directing effect on the crystal form obtained after sublimation and recondensation, we cannot say.

It is well-known that solvents can have a dramatic effect on crystal polymorphism, and glycine is a good example where “addition of methanol or ethanol to aqueous solutions induces the precipitation of the least stable β form of glycine”, whereas the thermodynamically more stable α - and γ -glycine forms crystallize from aqueous solution.^{71,72} Weissbuch et al. suggest

(70) The prediction that aspirin has two possible almost equi-energetic stackings of its sheet structure (Ouvrard, C.; Price, S. L. *Cryst. Growth Des.* **2004**, *4*, 1119) correlates with the observation of intergrowth of domains of both polymorphs (Bond, A. D.; Boese, R.; Desiraju, G. R. *Angew. Chem., Int. Ed.* **2006**), and a disordered crystal polymorph of chlorothalonil can be rationalized (Tremayne, M.; Grice, L.; Pyatt, J. C.; Seaton, C. C.; Kariuki, B. M.; Tsui, H. H. Y.; Price, S. L.; Cherryman, J. C. *J. Am. Chem. Soc.* **2004**, *126*, 7071) as arising from two low-energy layers structures with different stackings. There are many more low-energy interchangeable crystal structures for carbonic acid, and it is crystallized at significantly lower temperatures, so it is more likely to form an amorphous rather than a simple disordered state.

(71) Weissbuch, I.; Torbeev, V. Y.; Leiserowitz, L.; Lahav, M. *Angew. Chem., Int. Ed.* **2005**, *44*, 3226.

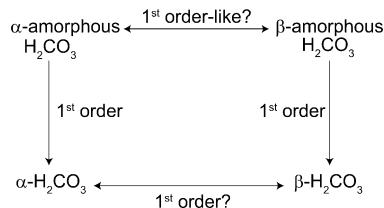
(72) Torbeev, V. Y.; Shavit, E.; Weissbuch, I.; Leiserowitz, L.; Lahav, M. *Cryst. Growth Des.* **2005**, *5*, 2190.

that various factors should be considered to understand the effect of solvent on crystal polymorphism, “for example the formation of structured clusters in solution prior to crystallization, the structure of growing surfaces that delineate emerging nuclei, the interaction between these surfaces and the solvent, as well as solvent–solute and solute–solute interactions.”⁷¹ and they conclude that “removal of the solvent molecules is an important rate-determining step in the growth of a given face.” FTIR spectroscopic studies by Davey et al. recently have shown for the first time a direct relationship between the assembly of molecules in solution and the solid form which crystallizes:^{73,74} solutions of tetrolic acid rich in dimers nucleate the α -polymorph, whereas solutions in more polar solvents, where dimer formation is disrupted, nucleate the catemeric β -polymorph. These studies also demonstrated the application of IR spectroscopy in in-situ studies for understanding the relationship between solution and solid-state interactions on crystallization. Such detailed studies are not experimentally feasible for carbonic acid. However, it seems clear that the solvent, methanol or water, has a directing effect on H-bond connectivity probably via the conformational state *a* in the two amorphous states and in the subsequently formed crystal polymorphs.

A crystalline CH_3OH adduct or a hydrate could be a precursor to formation of α - or β - H_2CO_3 , and because of that we have searched from the beginning of our studies on H_2CO_3 for these but without success.⁷⁵ A CH_3OH adduct as precursor to α - H_2CO_3 would be easily recognizable by intense CH_3OH bands in the CH and CO stretching band region,¹⁹ whereas a crystalline hydrate is expected to show OH stretching bands between 3550 and 3200 cm^{-1} which sharpen at low temperatures.^{76,77} In several of our experiments, films obtained by reaction of KHCO_3 with HCl or HBr aqueous solution were cooled to 78 K at various stages of the experiments, that is, for fully amorphous, partially crystalline, and fully crystalline films.²¹ In none of these experiments could sharp OH stretching bands assignable to a crystalline hydrate of β - H_2CO_3 be observed. The only sharp bands observable in this spectral region could be assigned to the hexahydrate of HCl (HBr),⁷⁸ to the dihydrate of NaCl (when using sodium salts), or to a mixed hydrate of CsCl (for Cs salts).⁷⁹ This shows that crystalline hydrates can, in principle, be formed under these experimental conditions.²¹

First-Order-Like Phase Transition? We next discuss the relation between the two amorphous states of H_2CO_3 called α -amorphous H_2CO_3 and β -amorphous H_2CO_3 (Scheme 1). The relative stability of the two crystalline phases is unclear and may well depend on thermodynamic variables. We have reported that β - H_2CO_3 transforms partly into α - H_2CO_3 on treatment with $\text{CH}_3\text{OH}/\text{HCl}$ and because of that have tentatively suggested that α - H_2CO_3 is the thermodynamically more stable form.²⁰ However, we cannot rule out that β - H_2CO_3 simply dissolves on

Scheme 1. First-Order-Like Phase Transition between α -Amorphous and β -Amorphous H_2CO_3 Deduced from Phase Transitions between Amorphous and Crystalline Forms of H_2CO_3



treatment with $\text{CH}_3\text{OH}/\text{HCl}$ and that α - H_2CO_3 forms only from the methanolic solution after pumping off $\text{CH}_3\text{OH}/\text{HCl}$. At 200 K, the rate of sublimation of α - H_2CO_3 was determined as $1.10^{-8} \text{ g cm}^{-2} \text{ s}^{-1}$ (see ref 24 and footnote 17 therein). At this temperature, β - H_2CO_3 does not show measurable sublimation, and thus, it is much lower than that of α - H_2CO_3 . An estimate for the saturation vapor pressure can be obtained from the sublimation rate by using the Knudsen formula.^{24,80} According to this estimate, α - H_2CO_3 has a higher vapor pressure at 200 K than β - H_2CO_3 and, thus, would be less stable than β - H_2CO_3 . Direct conversion of the two crystal polymorphs in the absence of solvent could not be observed at ≤ 200 K and 1 bar, that is, in the low-temperature range accessible without decomposition, and it seems doubtful for kinetic reasons whether this will ever be possible. Thus, we do not know whether the relationship between α - and β - H_2CO_3 is enantiotropic or monotropic, as expressed in a free energy versus temperature diagram.⁸¹ Organic crystal polymorphs are usually connected via a first-order phase transition,⁸¹ and the evidence above supports this assumption for α - and β - H_2CO_3 . The phase transition from both the α -amorphous and the β -amorphous state to α - and β - H_2CO_3 is expected to be first-order. It then follows that the α - and β -amorphous states are also connected by a first-order-like phase transition. An “apparently first-order transition between two amorphous phases of ice” (that is, high-density and low-density amorphous ice) was first postulated in 1985 by Mishima et al.³⁷ Since then, many examples for first-order-like phase transitions between amorphous states with different short-range order/intermediate-range order structural types and thermodynamic properties have been reported that are analogous to the crystal–crystal transitions (reviewed in ref 40). That is, the two amorphous states are separated by major energy barriers and can be treated as “phases”. Another scheme similar to Scheme 1 could be drawn for calcium carbonate where the amorphous calcium carbonate phase in larval snail shells has the short-range order of aragonite before it crystallizes,⁴¹ whereas the amorphous calcium carbonate phase transforming in sea urchin embryos into calcite has already the short-range order of calcite (see Introduction).^{42,43} The two crystal polymorphs calcite and aragonite apparently are connected via a first-order phase transition,^{82,83} and thus the two distinct amorphous calcium carbonate states seem also connected by a first-order-like phase transition.

(73) Parveen, S.; Davey, R. J.; Dent, G.; Pritchard, R. G. *Chem. Commun.* **2005**, 1531.

(74) Davey, R. J.; Dent, G.; Mughal, R. K.; Parveen, S. *Cryst. Growth Des.* **2006**, *6*, 1788.

(75) Hage, W. Isolierung von reiner Kohlensäure und deren FTIR-spektroskopische Charakterisierung mit Hilfe einer neuartigen Tieftemperaturmethode. Ph.D. Thesis, Universität Innsbruck, 1995.

(76) Nakamoto, K. *Infrared and Raman Spectra of Inorganic and Coordination Compounds*, 4th ed.; Wiley: New York, 1986.

(77) Falk, M.; Knop, O. Water in Stoichiometric Hydrates. In *Water a Comprehensive Treatise*; Franks, F., Ed.; Plenum Press: New York, 1973; Vol. 2, p 55.

(78) Ritzhaupt, G.; Devlin, J. P. *J. Phys. Chem.* **1991**, *95*, 90.

(79) Maki, A. G.; West, R. *Inorg. Chem.* **1963**, *3*, 657.

(80) Umrath, W. *Mikroskopie* **1983**, *40*, 9.

(81) Bernstein, J. *Polymorphism in Organic Crystals*; Clarendon: Oxford, 2002.

(82) Zimmermann, H. D. *Nature* **1971**, *231*, 203.

(83) Topor, N. D.; Tolokonnikova, L. I.; Kadenatsi, B. M. *J. Thermal Analysis* **1981**, *20*, 169.

(84) Mercury, CCDC. http://www.ccdc.cam.ac.uk/products/csd_system/mercury/ (accessed May 14, 2007).

Conclusions

We show by FTIR spectroscopy and X-ray diffraction that the precursors of the two crystal polymorphs of carbonic acid, α - and β -H₂CO₃, are two distinct amorphous states. It indicates that the two amorphous states are separated by potential energy barriers which are higher than those to their crystalline states. It is plausible that this type of behavior is much more general and that it occurs in many other systems. Furthermore, from comparison of IR spectra of α - and β -H₂CO₃ with those of their amorphous forms, we conclude that the two distinct H-bonding motifs observable in the crystalline phases exist already in the amorphous forms but without the translational symmetry and long-range order of the crystalline phases. Our computational polymorph search provides a plausible rationalization for these observations: we find a vast number of low-energy structures showing a variety of locally ordered hydrogen-bonded sheets and 3D networks for both low-energy conformers of carbonic

acid which are very close in energy. The two sets of reaction conditions with methanol or water as solvent may generate different conformations of the molecule as the growth units of the solid phase, which readily form an amorphous state. These conformations are likely retained upon crystallization.

Acknowledgment. We gratefully acknowledge financial support by the Austrian Science Fund (project P18187) and the British Council Academic Research Collaboration program. The Basic Technology program of the Research Councils UK funded “Control and Prediction of the Organic Solid State” (CPOSS, www.cposs.org.uk) which provided the infrastructure for the computational work. The computed crystal structures for carbonic acid are stored on CCLRC e-Science Centre data portal and are available on request.

JA073594F